PHYSICAL REVIEW B **82**, 045415 (2010)

Ab initio thermodynamics of deposition growth: Surface terminations of TiC(111) and TiN(111) grown by chemical vapor deposition

Jochen Rohrer* and Per Hyldgaard
BioNano Systems Laboratory, Department of Microtechnology, MC2, Chalmers University of Technology, SE-412 96 Gothenburg, Sweden
(Received 19 March 2010; revised manuscript received 11 June 2010; published 20 July 2010)

We present a calculational method to predict terminations of growing or as-deposited surfaces as a function of the deposition conditions. Such characterizations are valuable for understanding catalysis and growth phenomena. The method combines *ab initio* density-functional-theory calculations and experimental thermodynamical data with a rate-equations description of partial pressures in the reaction chamber. The use of rate equations enables a complete description of a complex gas environment in terms of a few, (experimentally accessible) parameters. The predictions are based on comparisons between free energies of reaction associated with the formation of surfaces with different terminations. The method has an intrinsic nonequilibrium character. In the limit of dynamic equilibrium (with equal chemical potential in the surface and the gas phase) we find that the predictions of the method coincide with those of standard *ab initio* based equilibrium thermodynamics. We illustrate the method for chemical vapor deposition of TiC(111) and TiN(111), and find that the emerging termination can be controlled both by the environment and the growth rate.

DOI: 10.1103/PhysRevB.82.045415 PACS number(s): 68.55.A−, 81.15.−z, 68.35.Md, 05.70.Ln

I. INTRODUCTION

The structure and chemical composition of surfaces play a fundamental role in many industrial applications. Identifying and ultimately learning to control surface terminations is a key issue in modern materials design. In heterogeneous catalysis[1] chemical reactions typically take place on the solid surface of the catalyst. Surfaces with different chemical compositions, for example, different surface terminations, support different chemical reactions.[2–4] This is true even if the exposed surfaces possess identical crystallographic orientations. Similarly, surface terminations strongly influence nucleation and growth processes. Different surface terminations do, in general, favor adsorption of different atomic species[5–7] and therefore affect subsequent growth of multicomponent materials.

Atomistic modeling[8–12] is highly valuable for design of functional materials and surfaces. It serves as an important complement to and extension of experimental characterizations. It also provides predictive power and thus an opportunity to accelerate innovation.[13] Coupling density-functional theory (DFT) to either thermodynamic[14–18] or kinetic modeling[19–22] has proven extremely useful for interpreting and complementing experimental techniques in characterization of surfaces,[23] thin films,[24] and interfaces.[25] Such modeling is often well-suited for descriptions of structures that are fabricated or investigated under well-controlled conditions, such as ultrahigh vacuum (UHV) or molecular beam epitaxy[26] (MBE).

Industrial mass production of materials often employ more efficient but less-controlled deposition methods, for example, chemical vapor deposition (CVD).[27] Such methods give rise to compositions and structures that need not be stable in a thermodynamical sense under ambient or UHV conditions. The fast deposition causes a lot more complexity in the growth process than is found in MBE. For example, it causes cluster formation and formation of intermediates in the gas phase or on the substrate and these structures define barriers for subsequent deposition events. Relevant experimental characterizations of surface terminations in such cases are difficult and require *in situ* measurements. Atomistic, *ab initio* based modeling is consequently of even higher value for as-deposited structures. However, a simple scale-up of the kinetic modeling[19–22] faces enormous practical problems because complex, unknown, and constantly evolving transition states determine the kinetics of the deposition.

In this paper, we propose an *ab initio* thermodynamics (AIT) method for deposition growth (hereafter referred to as AIT-DG). Our method combines DFT calculations with thermodynamic concepts and rate equations. The latter effectively describe supply and exhaust of gases to and from a reaction chamber as well as deposition processes inside. Steady-state solutions of these rate equations enable us to determine Gibbs free energies of reaction[28] of deposition processes that lead to different surface terminations. The free energies of reaction allow us to predict surface terminations as a function of the growth environment.

We emphasize that the AIT-DG method is fundamentally different from the *ab initio* thermodynamics method proposed in Refs. 15 and 16, also adapted to interfaces,[17] and used by many others. Such methods are designed to predict terminations of surfaces that are in *equilibrium* with a given gas environment (and are hereafter referred to as AIT-SE, *ab initio* thermodynamics with surface equilibrium). In contrast, our AIT-DG formulation possesses a nonequilibrium character, but formally contains the AIT-SE method in the regime, sometimes called dynamic equilibrium,[29] where one can assume equality of the chemical potentials in the surface and in the gas.

We illustrate the AIT-DG method for the CVD TiX(111) (X=C or N). These belong to the simplest class of materials where different surface terminations can arise. At the same time there is a high industrial interest in these materials. TiN is widely used as diffusion barrier for Al-based interconnects[30] and finds application as ohmic contact in GaN semiconductor technology.[31] TiC can be used as sub-

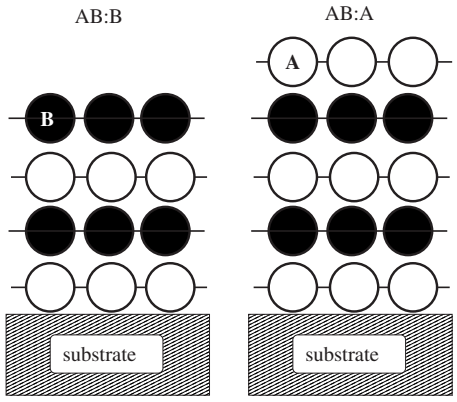

FIG. 1. Different surface terminations for a film deposited on a substrate. The schematics shows the case for a binary material AB formed of alternating A and B layers, represented by differently colored balls. While the interfacial composition largely is determined by the substrate properties, the composition of the surface layer strongly depends on the deposition environment, possibly leading to an AB film that slightly deviates from full stoichiometry.

strate for growth of other carbidic materials such as SiC or graphene[32] and its (111) surface also shows a potential as catalyst.[33] Moreover, TiC and TiN both are commonly used as Ti *X*/alumina multilayer coatings in cutting tool industry.[34]

The paper is organized as follows. Section II focuses on the discussion of surface terminations of binary materials. In Sec. III, we present our AIT-DG method in detail, exemplified for CVD of Ti*X*, and also considering the equilibrium limit of our method. Section IV summarizes the computational method that we use for all *ab initio* calculations. We present our results in Sec. V and discuss these as well as the method itself in Sec. VI. Section VII contains a summary and our conclusions.

II. SURFACE TERMINATIONS

Figure 1 shows a schematics of thin films of a binary material AB (deposited on a substrate) with the panels AB:A and AB:B differing essentially only by their surface terminations. Here and in the following, AB:A (AB:B) denotes an AB surface with A termination (B termination). The figure illustrates the character of our modeling where the difference in surface terminations is represented by films of different thicknesses; formally, the left panel represents a stoichiometric film grown to $2n$ layers while the right panel shows a nonstoichiometric film grown to $2n+1$ layers.[35] This case represents the simplest case of surfaces that can have more than one termination and the question arises which one will be created in a specific fabrication process.

Well-defined surface terminations can be created in a variety of different deposition methods, including the well-controlled MBE and less-controlled methods, such as CVD. MBE employs UHV and allows, in principle, one atom (or dimer) to be deposited at a time. An abrupt termination of the growth process therefore provides good explicit control over surface coverage and termination.

Less-controlled deposition methods typically yield much higher growth rates and are therefore more popular for large-scale manufacturing. In CVD, a substrate is exposed to an inflowing supply-gas mixture at high temperatures and at, compared to MBE, high pressures. Since there is no explicit control on the number of individual atoms or molecules in the gas environment or on the surface, one cannot simply end the deposition process so as to create a prespecified surface termination. A more involved analysis is necessary to understand what termination will emerge in deposition growth.

A. Materials example: TiC and TiN

Ti*X*(111) (*X*=C or N) are important, specific, examples where surface terminations have industrial relevance. Specifically, alternating deposition of Ti*X* and Al_2O_3 by CVD (Refs. 36 and 37) is commonly used to produce wear-resistant coatings on cemented-carbide cutting tools.[34]

The top panel of Fig. 2 illustrates the CVD process used for Ti*X* growth. A $TiCl_4$-CH_4-H_2-HCl [for TiC (Ref. 34)] or $TiCl_4$-N_2-H_2 [for TiN (Ref. 37)] supply gas mixture is injected into a CVD chamber via valve 1. The chamber is kept at a high constant temperature and at a constant pressure. The overall reactions that lead to the deposition of Ti *X* are

$$TiCl_4 + CH_4 \rightarrow TiC + 4HCl, \tag{1a}$$

$$TiCl_4 + \frac{1}{2}N_2 + 2H_2 \rightarrow TiN + 4HCl. \tag{1b}$$

Unused supply gas as well as reaction products are exhausted from the chamber via valve 2.

In Ti*X*/alumina multilayers, the Ti *X*(111) surface terminations play a crucial role for the nucleation of alumina and consequently for the nature of the Ti*X*/alumina interface in the coatings. In particular, Ti-terminated surfaces indicate an interface composition of the type $TiX:Ti/O:Al_2O_3$, whereas *X*-terminated surfaces favor a $TiX:X/Al:Al_2O_3$ interface.[7,38,39] Here, $(O,Al):Al_2O_3$ specifies the dominant chemical species (O or Al) of alumina at the interface.

To the best of our knowledge, experimental studies on the Ti *X*(111) surface termination exist only for TiC (Refs. 40–42) but not for TiN. They all report a Ti-terminated surface. However, in all these experiments, the TiC(111) surface was prepared by high-temperature annealing (and associated selective evaporation) under UHV conditions. The observed Ti termination of the TiC(111) surface under such experimental conditions can be understood from a theoretical argument due to Tan *et al.*,[18] estimating the selective high-temperature evaporation from the total-energy cost of pulling atoms out of material.

A predictive, atomistic theory of the surface termination of as-deposited Ti*X*(111) as a function of the growth environment remains of central value. The characterizations and predictions are important, for example, to define a proper starting point for understanding atomistic processes in the fabrication of Ti*X*/alumina multilayer coatings.[36]

B. Kinetics of deposition processes

The bottom panel of Fig. 2 shows a schematics of the kinetics leading to a surface system with an excess Ti layer.

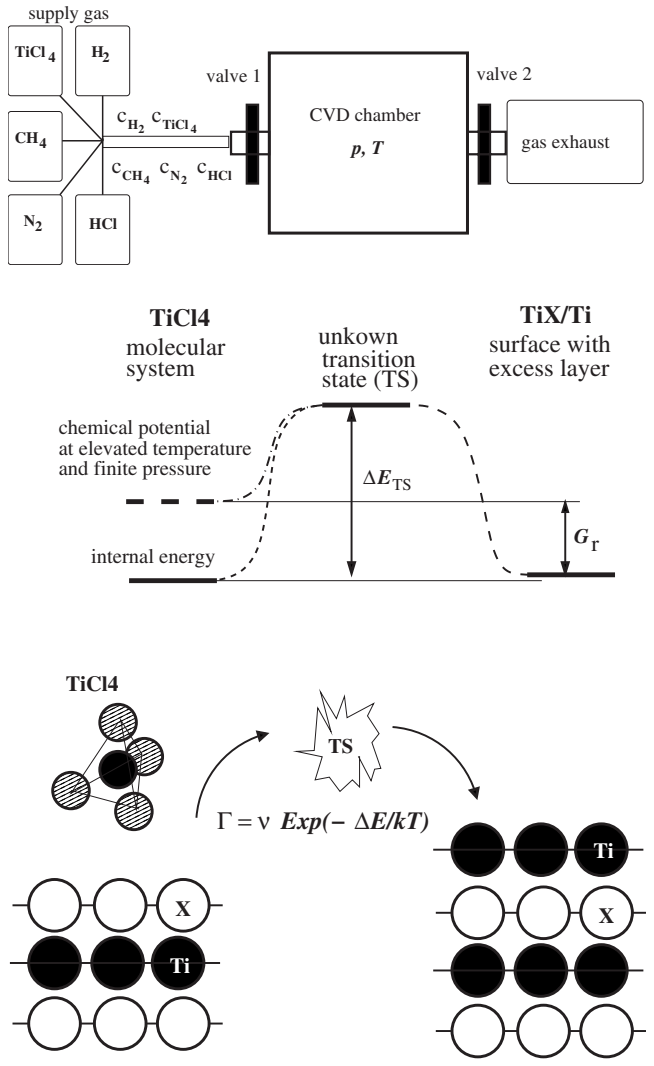

FIG. 2. Schematics of CVD of Ti*X* and of the kinetics in the formation of excess layers. *The upper panel* gives a principle sketch of a CVD apparatus. A supply gas mixture that contains several different gases with different concentrations c_i is injected into the CVD chamber via valve 1 at a rate R_{sup}. The chamber is kept at a constant temperature T and pressure p. Inside the chamber the gases react and form Ti*X*. Reaction products and unused supply gas are exhausted at a rate R_{exh} via valve 2. *The set of lower panels* illustrates kinetic effects that specify the surface termination. A Ti (X) surface layer can be deposited from a Ti (X) carrying gas, here shown for $TiCl_4$. As indicated, the process involves a set of unknown complex transition states.

The initial state is represented by a $TiCl_4$ molecule above the X-terminated TiX(111) surface. In the final state, a Ti atom (or a layer after a number of events) is deposited. Additional molecules that enter or leave the reaction and produce the final state are not shown. We also sketch the energy landscape as a function of a generic reaction coordinate. We note that only the relative energy positions of the initial and final states are shown in correspondence with the actual results of our modeling; the nature and energy of the relevant transition states are unknown.

Surface morphologies obtained in MBE growth can often by understood from kinetic Monte Carlo (kMC) simulations, using DFT calculations to determine process barriers.[19–22] Such simulations follow the surface morphology over some time by allowing for a number of events to take place at random. Conceptually it is simple to generalize the kMC approach to CVD but in practice such a generalization will be extremely challenging. The chemical species supplied in CVD are usually more complex than single atoms or dimers used in MBE. Worse, the reactants will not, in general, simply dissociate on the surface but enter into complicated reactions with other species and form clusters. These reactions are not limited to the surface and may lead to a large variety of intermediates. While adaptive intelligent kMC exists and is being developed,[22] the complexity in CVD is enormous.

At the same time, the high deposition temperature in CVD motivates a shift away from explicit kinetic modeling. We therefore develop a thermodynamic description that focuses entirely on initial and final states, retaining the simplicity of the analysis for selective evaporation in UHV.[18] A nonequilibrium thermodynamic description becomes applicable when high temperature facilitates structural reorganization and permits the growing system to reach and sample the set of possible final states.

C. Excess-layer deposition

Figure 3 illustrates possible processes that lead to deposition of single Ti and C layers for TiC. We determine a preference for the surface termination by comparison of the Gibbs free energy of reaction for such excess-layer structures with those of the stoichiometric TiX. The reactions listed in Eq. (1) only describe deposition that leads to TiX with the full stoichiometry of the bulk. We supplement that description by a thermodynamic characterization of dominant reaction pathways leading to formation of excess layers for both TiC and TiN systems.

For excess-layer reactions, we consider the following reactions for Ti deposition on TiC and TiN

$$\text{TiC:C} + \text{TiCl}_4 + 2\text{H}_2 \rightarrow \text{TiC:C/Ti} + 4\text{HCl}, \tag{2a}$$

$$\text{TiN:N} + \text{TiCl}_4 + 2\text{H}_2 \rightarrow \text{TiN:N/Ti} + 4\text{HCl}. \tag{2b}$$

Here, TiC:C/Ti (TiN:N/Ti) identifies a system with an additional Ti layer on the C-terminated TiC (N-terminated TiN) surface. Additional X layers may be deposited as

$$\text{TiC:Ti} + \text{CH}_4 \rightarrow \text{TiC:Ti/C} + 2\text{H}_2, \tag{3a}$$

$$\text{TiN:Ti} + \frac{1}{2}\text{N}_2 \rightarrow \text{TiN:Ti/N}. \tag{3b}$$

Since deposition of Ti is relevant only on an X-terminated surface and deposition of X only on the Ti-terminated surface we suppress the specification of the original surface termination in the following. For example, TiC/Ti will be used instead of TiC:C/Ti.

III. *AB INITIO* THERMODYNAMICS OF DEPOSITION GROWTH

Our thermodynamic method to predict terminations of growing surfaces describes phenomena that lie between the

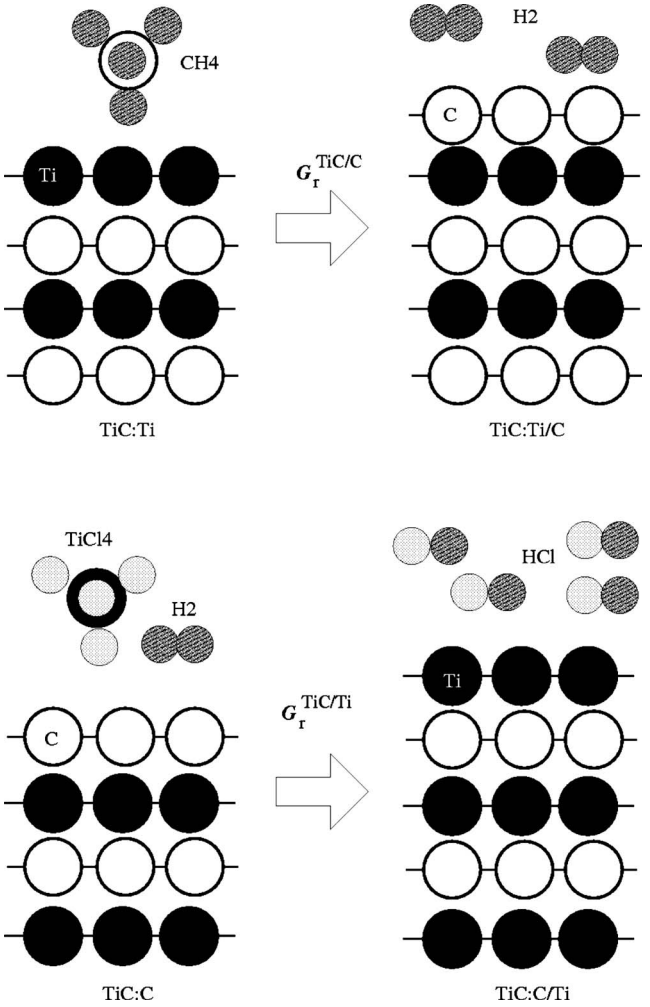

FIG. 3. Formation of excess layers and associated free energies of reaction G_r. The top panel illustrates the formation of a C excess layer from CH_4 on a Ti-terminated surface. The bottom panel shows the formation of a Ti excess layer from $TiCl_4$ and H_2 on a C-terminated surface. From a kinetic perspective, formation of specific clusters and presence of H_2 may catalyze the process shown in the upper panel; thermodynamically, such catalytic processes do not, however, affect the free energy of reaction.

static equilibrium limit and the nonequilibrium limit that requires a fully kinetic theory. We assume an experimental setup similar to that illustrated in the top panel of Fig. 2.

A. Computational strategy and assumptions

We use the difference in Gibbs free energies of reaction

$$\Delta G_r^{AB} = G_r^A - G_r^B \tag{4}$$

as a predictor for the prevalence of growing either an A-terminated ($\Delta G_r^{AB} < 0$) or a B-terminated ($\Delta G_r^{AB} > 0$) surface of a binary material AB. Here, $G_r^{A(B)}$ is the free energy of reaction associated with the formation of an excess A (B) layer. Our choice of predictor follows naturally from an analogy with chemical reaction theory[28,29] and from considering surface transformations. The following coupled set of reactions change an A- (B-) terminated AB surface into a B- (A-) terminated surface

$$\mathrm{I{:}B} + \mathrm{React_I} \underset{\Gamma_b^I}{\overset{\Gamma_f^I}{\rightleftharpoons}} \mathrm{A} + \mathrm{Prod_I}, \tag{5a}$$

$$\mathrm{II{:}A} + \mathrm{React_{II}} \underset{\Gamma_b^{II}}{\overset{\Gamma_f^{II}}{\rightleftharpoons}} \mathrm{B} + \mathrm{Prod_{II}}. \tag{5b}$$

The probability for growing either an A- or B-terminated surface is described by rate equations where the rates $\Gamma_{\{f,b\}}^{\{I,II\}}$ depend on the deposition environment (reactants $\mathrm{React}_{\{I,II\}}$ and products $\mathrm{Prod}_{\{I,II\}}$). The steady-state solution $P_A/P_B = (\Gamma_f^I + \Gamma_b^{II})/(\Gamma_b^I + \Gamma_f^{II})$ is closely approximated by

$$P_A/P_B \approx \exp(-\beta \Delta G_r^{AB}/2), \tag{6}$$

where β denotes the inverse temperature. This evaluation in Eq. (6) becomes exact in the limit of dynamic equilibrium (identified by $G_r^A + G_r^B = 0$) where ΔG_r^{AB} reduces to a difference in surface free energies. Further details on the nature of the strategy and the applicability to nonequilibrium conditions are given in the Appendix.

The assumptions that facilitate the evaluation of free energies of reaction are: (1) the system composed of the growing surface and the gas environment settles into a steady state, specified by the gas supply, deposition, and gas exhaust rates. We do not *a priory* assume that the gases and the surface are in mutual equilibrium, nor do we generally expect such an equilibrium to emerge. (2) Each of the gases that take part in reactions is fully thermalized at the steady-state partial pressure so that we can associate a chemical potential to them. (3) The overall pressure is low enough so that a description of all gases in terms of the ideal-gas approximation applies. (4) The temperature of the system is high enough so that we can neglect kinetic barriers.

The computational strategy and the first assumption of a steady state is a central feature of our method. We derive the steady state from a rate equation that describes the supply and exhaust of gases into and from the reaction chamber as well as the deposition inside the chamber.

The other three assumptions are identical to those of the AIT-SE method. The AIT-SE describes a system in a static equilibrium at high temperatures. The AIT-SE might also describe systems in *dynamic equilibrium*. Dynamic equilibrium[29] here means that the free energy of reaction (derived and calculated below) exactly equals zero. This condition also applies in static equilibrium but in dynamic equilibrium the zero value of the free energy of reaction arises from the steady-state concentrations of reactants and reaction products. A (virtual) drop in the reaction rate readily leads to a drop of the concentrations of reaction products but not of the reactants (due to the supply and exhaust) so that the dynamics of the reaction is restored.

We find that as the steady state approaches dynamic equilibrium, the predictions of AIT-DG coincide with those of the AIT-SE. However, even if dynamic equilibrium is reached, our description in terms of a rate equation will be necessary in order to determine chemical potentials of the gas-phase

constituents from their individual pressures during the process. We also emphasize that, during growth, the steady state does not necessarily settle into a state of dynamic equilibrium.

B. Excess layers and their free energies of reaction

Figure 3 illustrates the formation of Ti and C excess layers on TiC(111), corresponding to the reactions in Eqs. (2a) and (3a). Similarly, we assume that Ti and N excess layers can be deposited on TiN(111) according to the reactions in Eqs. (2b) and (3b).

We represent the TiX(111) surface before deposition of additional layers by a stoichiometric slab. Upon deposition of an additional layer the slab becomes nonstoichiometric, which motivates the terminology of an excess layer. A stoichiometric TiX(111) slab is asymmetric along the [111] direction. In particular, it possesses one Ti-terminated surface and one X-terminated surface. An excess Ti layer is deposited on the X-terminated side of the slab while an excess X layer is be deposited on the Ti-terminated side.

We introduce the chemical potentials $\mu_{\mathrm{Ti}}^{\mathrm{aig}}$, $\mu_{\mathrm{C}}^{\mathrm{aig}}$, and $\mu_{\mathrm{N}}^{\mathrm{aig}}$ for Ti, C, and N atoms in the gases. The set of μ_i^{aig} can be conveniently related to differences between several molecular chemical potentials (see below). The chemical potentials of Ti, C, and N in the gases do not in general equal the respective chemical potentials μ_{Ti}, μ_{C}, and μ_{N} in the solid bulk. For the latter the free energy per bulk unit,[43] $g_{\mathrm{Ti}\,X}$, always specifies material stability

$$\mu_{\mathrm{Ti}} + \mu_X = g_{\mathrm{Ti}X}. \tag{7}$$

Growth of TiX, on the other hand, is characterized by

$$g_{\mathrm{Ti}X} < \mu_{\mathrm{Ti}}^{\mathrm{aig}} + \mu_X^{\mathrm{aig}}. \tag{8}$$

The free energy of reaction[28] for the deposition of one unit of bulk is defined as

$$g_{\mathrm{r}}^{\mathrm{Ti}X} = g_{\mathrm{Ti}X} - \mu_{\mathrm{Ti}}^{\mathrm{aig}} - \mu_X^{\mathrm{aig}}. \tag{9}$$

We also introduce the free energy of reaction G_{r} which corresponds to the gain in energy per surface unit in the deposition of one excess layer. For deposition of excess Ti, G_{r} can then be written as[44]

$$G_{\mathrm{r}}^{\mathrm{TiC/Ti}} = G_{\mathrm{TiC/Ti}} - G_{\mathrm{TiC}} - \mu_{\mathrm{Ti}}^{\mathrm{aig}}, \tag{10a}$$

$$G_{\mathrm{r}}^{\mathrm{TiN/Ti}} = G_{\mathrm{TiN/Ti}} - G_{\mathrm{TiN}} - \mu_{\mathrm{Ti}}^{\mathrm{aig}}. \tag{10b}$$

Here, $G_{\mathrm{Ti}X}$ is the free energy of a stoichiometric, nonsymmetric TiX slab and $G_{\mathrm{Ti}X/\mathrm{Ti}}$ denotes the free energy of the system that consists of the same stoichiometric TiX slab and an additional Ti excess layer (adsorbed on the X-terminated side of the slab). For excess X, the free energy of reaction is given by

$$G_{\mathrm{r}}^{\mathrm{TiC/C}} = G_{\mathrm{TiC/C}} - G_{\mathrm{TiC}} - \mu_{\mathrm{C}}^{\mathrm{aig}}, \tag{11a}$$

$$G_{\mathrm{r}}^{\mathrm{TiN/N}} = G_{\mathrm{TiN/N}} - G_{\mathrm{TiN}} - \mu_{\mathrm{N}}^{\mathrm{aig}}. \tag{11b}$$

With these definitions, a negative value of G_{r} implies that the deposition of the excess layer is thermodynamically favorable and that the reaction proceeds in the direction of the arrow in one of the listings in Eqs. (2) and (3). A positive value of G_{r} implies that the deposition of the corresponding excess layer is thermodynamically unfavorable and that the reaction proceeds in the opposite direction.

The atom-in-gas chemical potentials μ_i^{aig} depend on the composition of the environment and can therefore be controlled by the gas flow. For the case of CVD of TiX with the here-considered supply gas and the reactions listed in Eqs. (2) and (3), we assign the atomic chemical potentials in the gas as

$$\mu_{\mathrm{Ti}}^{\mathrm{aig}} = \mu_{\mathrm{TiCl_4}} + 2\mu_{\mathrm{H_2}} - 4\mu_{\mathrm{HCl}}, \tag{12a}$$

$$\mu_{\mathrm{C}}^{\mathrm{aig}} = \mu_{\mathrm{CH_4}} - 2\mu_{\mathrm{H_2}}, \tag{12b}$$

$$\mu_{\mathrm{N}}^{\mathrm{aig}} = \frac{1}{2}\mu_{\mathrm{N_2}}. \tag{12c}$$

We note that, in general, the deposition of excess Ti followed by the deposition of excess X (or vice versa) equals the free energy of reaction for the deposition of one unit of bulk

$$G_{\mathrm{r}}^{\mathrm{Ti}X/\mathrm{Ti}} + G_{\mathrm{r}}^{\mathrm{Ti}\,X/X} = g_{\mathrm{r}}^{\mathrm{Ti}X}. \tag{13}$$

If the solid-gas system approaches *equilibrium* (mediated through the surface), we have $g_{\mathrm{r}}^{\mathrm{Ti}X}=0$ so that the reaction energy gain is simply

$$G_{\mathrm{r}}^{\mathrm{Ti}X/\mathrm{Ti}} + G_{\mathrm{r}}^{\mathrm{Ti}X/X} = 0. \tag{14}$$

We emphasize that the definitions in Eqs. (10) and (11) do not make any assumption about equilibrium. On the contrary, by calculating Eq. (13) as a function of deposition pressure and temperature, we can predict whether the process is in or out of equilibrium, and in which direction it proceeds.

C. Gibbs free energies and chemical potentials

Calculating free energies of reactions requires simple approximations to evaluate free energies of surface systems and chemical potentials of gas-phase species. We base these approximations on experimentally available thermochemical data.

For the gases, we employ the ideal gas approximation. This approximation in justified for low pressures which is typically the case in CVD of TiX. It also allows us to express the μ_i in terms of temperature T and partial pressure p_i

$$\mu_i(T,p_i) = \epsilon_i + \Delta_i^0(T) + k_B T \ln(p_i/p^0). \tag{15}$$

Here ϵ_i is the DFT total energy of the gas phase species (molecule) and k_B is the Boltzmann constant. $\Delta_i^0(T)$ is the temperature dependence of μ_i at a fixed pressure p^0, and related to enthalpy and entropy differences.[16] The latter are available for $p^0=1$ atm for many molecules in thermochemical tables such as Ref. 45.

For surface systems, we approximate the Gibbs free energy by the DFT total energy

$$G \approx E, \tag{16}$$

where G and E stand for one of $G_{\mathrm{Ti}X/\mathrm{Ti}}$ and $E_{\mathrm{Ti}X/\mathrm{Ti}}$ or $G_{\mathrm{Ti}\,X/X}$ and $E_{\mathrm{Ti}X/X}$. This approximation neglects vibrational contributions (TS^{vib}) and the pressure term (pV) in G. However, the effect of neglecting these factors is expected to be small.[16,46]

D. Rate equation and steady-state solution

Evaluation of the gas-phase chemical potentials in Eq. (15) requires the specification of the deposition temperature and the individual partial pressures. The temperature and the total pressure inside the CVD chamber can be controlled reasonably well during fabrication. Individual partial pressures, on the other hand, are not directly accessible. However, they can be determined from a rate equation that describes the overall CVD process.

Using the ideal gas approximation ($pV=Nk_BT$), the change in individual pressures is described by

$$\partial_t p_i(t) = \frac{k_B T}{V_{\mathrm{CVD}}}\left[c_i R_{\mathrm{sup}} - \frac{p_i(t)}{p(t)} R_{\mathrm{exh}} + \nu_i R_{\mathrm{Ti}X}\right], \tag{17}$$

where $p(t)=\Sigma_i p_i(t)$ is the total pressure, $p_i(t)$ denotes the partial pressure of species i at time t, and ν_i is the corresponding stoichiometric coefficient (change in number of molecules) in the deposition process, Eq. (1). Per definition,[28] stoichiometric coefficients are negative for species that are consumed in the reaction and positive for reaction products. The value of c_i reflects the concentration of species i in the supply gas. Finally, R_{sup} and R_{exh} are the rates at which the gases are supplied to and exhausted from the chamber; $R_{\mathrm{Ti}\,X}$ is the rate of TiX deposition (per stoichiometric formula).

In steady state, we can eliminate either one of the three rates. Keeping the supply and deposition rate as fundamental variables, the steady-state solution ($\partial_t p=0$ and $\partial_t p_i=0$) of Eq. (17) is given by

$$p_i = p\frac{c_i + \nu_i r_{\mathrm{Ti}X}}{1 + \Delta\nu r_{\mathrm{Ti}X}}. \tag{18}$$

Here, p and p_i (without time argument) denote the steady-state total (which can be controlled) and partial pressures and $\Delta\nu=\Sigma\nu_i$ is the number of molecules that are created in each reaction. We have also introduced the scaled TiX deposition rate $r_{\mathrm{Ti}X}=R_{\mathrm{Ti}X}/R_{\mathrm{sup}}$.

Collecting Eqs. (10), (11), (15), (16), and (18), we can express the Gibbs free energy of reaction for deposition of excess layers as a function of three variables: the temperature T, the pressure p, and the scaled Ti X deposition rate $r_{\mathrm{Ti}\,X}$

$$G_{\mathrm{r}} = G_{\mathrm{r}}(\{\mu_i[T,p_i(r_{\mathrm{Ti}X})]\}) = G_{\mathrm{r}}(T,p,r). \tag{19}$$

Here G_{r} denotes one of $G_{\mathrm{r}}^{\mathrm{Ti}X/\mathrm{Ti}}$ or $G_{\mathrm{r}}^{\mathrm{Ti}X/X}$.

E. Limits on the scaled deposition rate

The scaled deposition rates r_{TiC} and r_{TiN} possess critical values $r_{\mathrm{TiC}}^{\mathrm{crit}}$ and $r_{\mathrm{TiN}}^{\mathrm{crit}}$, i.e., upper values for the parameter r that are still compatible with actual growth. Deposition of TiX is favorable only if the inequality in Eq. (8) holds. For $r_{\mathrm{Ti}X} \geq r_{\mathrm{Ti}X}^{\mathrm{crit}}$, the accumulation of reaction products makes the reaction thermodynamically unfavorable. Thus, in a steady state, $r_{\mathrm{Ti}\,X} \leq r_{\mathrm{Ti}X}^{\mathrm{crit}}$ must be fulfilled whereas equality corresponds to (dynamic) equilibrium. This leads to the conditions

$$g_{\mathrm{TiC}} \equiv \mu_{\mathrm{TiCl}_4}(r_{\mathrm{TiC}}^{\mathrm{crit}}) + \mu_{\mathrm{CH}_4}(r_{\mathrm{TiC}}^{\mathrm{crit}}) - + 4\mu_{\mathrm{HCl}}(r_{\mathrm{TiC}}^{\mathrm{crit}}), \tag{20a}$$

$$g_{\mathrm{TiN}} \equiv \mu_{\mathrm{TiCl}_4}(r_{\mathrm{TiN}}^{\mathrm{crit}}) + 2\mu_{\mathrm{H}_2}(r_{\mathrm{TiN}}^{\mathrm{crit}}) + \frac{1}{2}\mu_{\mathrm{N}_2}(r_{\mathrm{TiN}}^{\mathrm{crit}}) - 4\mu_{\mathrm{HCl}}(r_{\mathrm{TiN}}^{\mathrm{crit}}), \tag{20b}$$

using $\mu_i(r_{\mathrm{Ti}X}^{\mathrm{crit}})=\mu_i(T,p[r_{\mathrm{Ti}X}^{\mathrm{crit}}])$ as shorthand. Critical values, i.e., upper limits for the scaled deposition rate, are identified by solving these equations.

F. Equilibrium limit

The AIT-DG method formally resembles the AIT-SE when taking the limit in which the gas environment is in equilibrium with the surface. Strictly speaking, the AIT-DG method expresses the same thermodynamic preference as does a generalization of the AIT-SE method to dynamic equilibrium. The dynamic equilibrium is nevertheless still specified by solving the rate equations for the steady-state gas flow.

We express the differences in reaction free energies for excess Ti and excess X surface layers as

$$G_{\mathrm{r}}^{\mathrm{Ti}X/\mathrm{Ti}} - G_{\mathrm{r}}^{\mathrm{Ti}X/X} = G_{\mathrm{Ti}X/\mathrm{Ti}} - \mu_{\mathrm{Ti}}^{\mathrm{aig}} - (G_{\mathrm{Ti}X/X} - \mu_X^{\mathrm{aig}}). \tag{21}$$

Equilibrium between the gas phase and the surface, Eq. (14), implies

$$0 = \mu_{\mathrm{Ti}}^{\mathrm{surf}} + \mu_X^{\mathrm{surf}} - \mu_{\mathrm{Ti}}^{\mathrm{aig}} - \mu_X^{\mathrm{aig}}, \tag{22}$$

where $\mu_{\mathrm{Ti}}^{\mathrm{surf}}=G_{\mathrm{Ti}X/\mathrm{Ti}}-G_{\mathrm{Ti}X}$ and $\mu_X^{\mathrm{surf}}=G_{\mathrm{Ti}X/X}-G_{\mathrm{Ti}X}$ are the chemical potentials of Ti and X at the surface of the solid.

If we also assume equilibrium between the bulk and the surface, that is, $\mu_{\mathrm{Ti}}^{\mathrm{surf}}+\mu_X^{\mathrm{surf}}=\mu_{\mathrm{Ti}}+\mu_X$, and use Eq. (7), we obtain

$$G_{\mathrm{r}}^{\mathrm{Ti}} - G_{\mathrm{r}}^{X} = G_{\mathrm{Ti}X/\mathrm{Ti}} - G_{\mathrm{Ti}X/X} - g_{\mathrm{Ti}X} + 2\mu_X^{\mathrm{aig}} \tag{23}$$

as a predictor of preference of *equilibrium* surface terminations.

This equilibrium predictor can be expressed in terms of a difference in surface free energies, thus making a connection to the AIT-SE (Ref. 47)

$$G_{\mathrm{r}}^{\mathrm{Ti}} - G_{\mathrm{r}}^{X} = 2A(\gamma^{\mathrm{Ti}X/\mathrm{Ti}} - \gamma^{\mathrm{Ti}X/X}). \tag{24}$$

Here, we use the standard definition of the surface free energy

$$\gamma^{\mathrm{Ti}\,X/\mathrm{Ti}} = \frac{1}{2A}(G_{\mathrm{Ti}X/\mathrm{Ti}} - n_1 g_{\mathrm{Ti}X} + \mu_X), \tag{25a}$$

$$\gamma^{\mathrm{Ti}\,X/X} = \frac{1}{2A}(G_{\mathrm{Ti}X/X} - n_2 g_{\mathrm{Ti}X} - \mu_X), \tag{25b}$$

for the Ti- and X-terminated surfaces, respectively. The numbers n_1 and n_2 correspond to the numbers of Ti layers in the

TABLE I. Calculated and experimental data for molecules relevant to CVD of TiX. Total energies are required for reference for the calculation of chemical potentials. Calculated geometric data, such as bond lengths b and bond angles θ, are in excellent agreement with the experimental one. Calculated atomization energies E_{atom} of N_2, H_2, and CH_4 differ only slightly from experimental values (we use the value of $E_{\mathrm{H}}=-13.6$ eV for the H atom in favor of the DFT value to calculate atomization energies of molecules that carry H). For Cl-containing molecules, the differences are larger.

	E_{atom} (eV/molecule)		ΔE_{atom}	b (Å)		Δb	θ (deg)	
Molecule	Present	Expt.[a]	(%)	Present	Expt.[a]	(%)	Present	Expt.[a]
H_2	4.58	4.48	2.2	0.75	0.741	1.2		
$TiCl_4$	21.31	17.84	19	2.18	2.17	0.05	109.5±2	109.471
N_2	9.63	9.76	1.3	1.12	1.098	2.0		
CH_4	18.23	17.02	7	1.10	1.087	1.2	109.5	109.471
HCl	4.88	4.43	10	1.29	1.275	1.2		

[a]Reference 52.

TiX/Ti and the TiX/X slabs so that $n_1-n_2=1$. In equilibrium, the difference in free energies of reaction is therefore simply the difference in surface free energies between the Ti- and X-terminated surface

At the same time, we emphasize that

$$\mu_{\mathrm{Ti}}+\mu_X=g_{\mathrm{Ti}X}\neq\mu_{\mathrm{Ti}}^{\mathrm{aig}}+\mu_X^{\mathrm{aig}} \tag{26}$$

applies for general growth conditions. A nonequilibrium-driven process such as growth will not generally adjust itself to dynamic equilibrium. Out of dynamic equilibrium, a prediction of surface terminations in terms of surface free energies (employing $\mu_X=\mu_X^{\mathrm{aig}}$) is not justified. Instead, the free energy of reaction is the proper quantity to use to predict surface terminations.

IV. COMPUTATIONAL METHOD

All DFT calculations are performed with the plane-wave code DACAPO (Ref. 48) using ultrasoft pseudopotentials,[49] the PW91 exchange-correlation functional,[50] and 400 eV plane-wave cutoff. The 1×1 TiX(111) surfaces are represented by slab geometry within a supercell including ~10 Å of vacuum. A $3\times3\times1$ Monkhorst-Pack k-point sampling[51] is used and atomic relaxations are performed until interatomic forces no longer exceed a value of 0.03 eV/Å. The slabs contain 12 Ti and 12 X layers for the stoichiometric reference surface without excess layer, 13 Ti and 12 X layers for the surface with Ti excess layer, and 12 Ti and 13 X layers for the surface with X excess layer. We have checked that the bulk energies per TiC unit, calculated as $\epsilon_{\mathrm{Ti}X}=E(N+1)-E(N)$, are converged to a difference of less than 0.03 eV with respect to the slab thickness. Here $E(N)$ and $E(N+1)$ is the energy of a TiX, TiX/Ti, or TiX/X slab that contains N and $N+1$ Ti layers, that is, the bulk energy is independent of the surface termination, as it should be.

For molecules and atoms, we use spin-polarized calculations when relevant. Total energies are calculated within unit cells of size $20\times20\times20$ Å^3, assuring that molecules from different cells do not interact. We use a $1\times1\times1$ Monkhorst-Pack k-point sampling[51] and perform atomic relaxations until interatomic forces no longer exceed a value of 0.01 eV/Å.

V. RESULTS

Table I lists the calculated atomization energies, bond lengths, and bond angles of molecules that are relevant for CVD of TiX. For atomization energies, our calculated values are in very good agreement for H_2 and N_2. For other molecules, we find larger discrepancies, in particular for $TiCl_4$. However, since the geometric properties are in excellent agreement with experiment, we suspect that these discrepancies are mainly related to total energies of the isolated atoms. We therefore trust total energies of the listed molecules as reference energies in the calculations of chemical potentials.

Figure 4 displays the critical scaled deposition rates $r_{\mathrm{Ti}X}^{\mathrm{crit}}$ as functions of temperature for two different pressures and two different concentrations of HCl in the supply gas. We

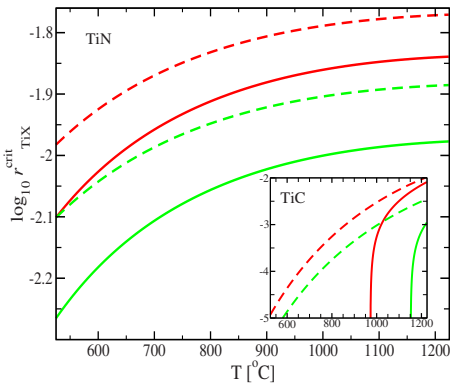

FIG. 4. (Color online) Critical values of the scaled reaction rate $r_{\mathrm{TiN}}^{\mathrm{crit}}$ as functions of temperature at different pressures and HCl concentrations. Red (dark) lines correspond to a deposition pressure of $p_1=50$ mbar and green (light) lines to $p_2=500$ mbar. Solid lines correspond to no HCl content $c_{\mathrm{HCl},1}=0$ in the supply gas, dashed lines to a content of 1% HCl $c_{\mathrm{HCl},1}=0.01$. The insert shows the corresponding analysis for TiC.

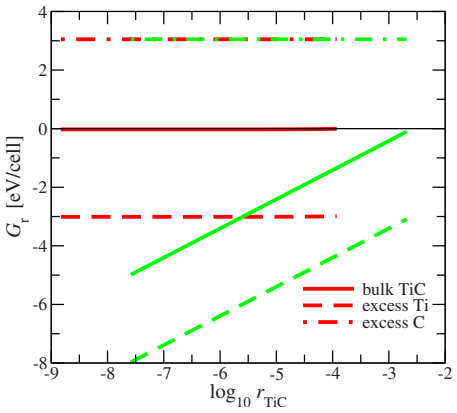

FIG. 5. (Color online) Free energies of reaction G_r of CVD bulk TiC (solid), excess Ti (dashed), and C excess layers (dashed-dotted) at the TiX(111) surface as a function of the scaled reaction rate r_{TiC}. We assume a total pressure of $p=50$ mbar and a deposition temperature of $T=980$ °C inside the CVD chamber. Red (dark) lines correspond to experimental values (Ref. 34) for the supply gas compositions, see also main text. In particular, the supply gas contains 1% HCl. The green (light) lines correspond to the case where no HCl is supplied.

find that r_{TiX}^{crit} first increases with increasing temperature and then approaches an asymptotic value. At fixed temperature, r_{TiX}^{crit} decreases with increasing total pressure. We also find a divergence in $\log_{10} r_{TiX}^{crit}(T)$ as the temperature decreases. This divergence can be seen most pronounced for TiC in the case where no HCl is supplied (divergences of other graphs lie outside the plotted regime). This divergence arises because lowering of the temperature below a certain value causes g_r^{TiX} to become positive for all choices of $r_{Ti\,X}$.

TiC(111). Fig. 5 reports the calculated free energies of reaction of Ti and C excess layers as well as the free energy of reaction of one stoichiometric unit of bulk TiC. We plot the free energies of reaction as functions of the scaled reaction rate r_{TiC} at fixed temperatures and pressures. The scaled reaction rate is limited to right by its critical value when dynamic equilibrium is reached, see Eq. (20). We assume experimental values for the supply gas composition as stated in Ref. 34. In detail, we have $c_{TiCl_4}=0.04$, $c_{CH_4}=0.07$, $c_{HCl}=0.01$, and $c_{H_2}=1-\Sigma_i x_i$.

We find that $G_r^{TiC/C} > G_r^{TiC/Ti}$ in the entire range of the scaled deposition rate r_{TiC}. Furthermore, the free energy of reaction associated with a C-terminated TiC(111) surface is positive. Thus, under the considered experimental circumstances, the TiC(111) surface will be Ti terminated.

We have also tested the consequences of varying deposition parameters. With the chosen set of supply gases, it was not possible to identify a set of deposition parameters that could lead to a favored C-termination of the TiC(111) surface. *TiN(111).* Fig. 6 reports the calculated free energies of reaction of Ti and N excess layers as well as the free energy of reaction of one stoichiometric unit of bulk TiN. In the upper panel, we assume experimental values for the supply gas composition as stated in Ref. 37. In detail, we have $x_{TiCl_4}=0.09$, $x_{N_2}=0.5$, and $x_{H_2}=1-\Sigma_i x_i$.

We find that the free energies of reactions of both excess Ti and excess N can be negative simultaneously. Far from

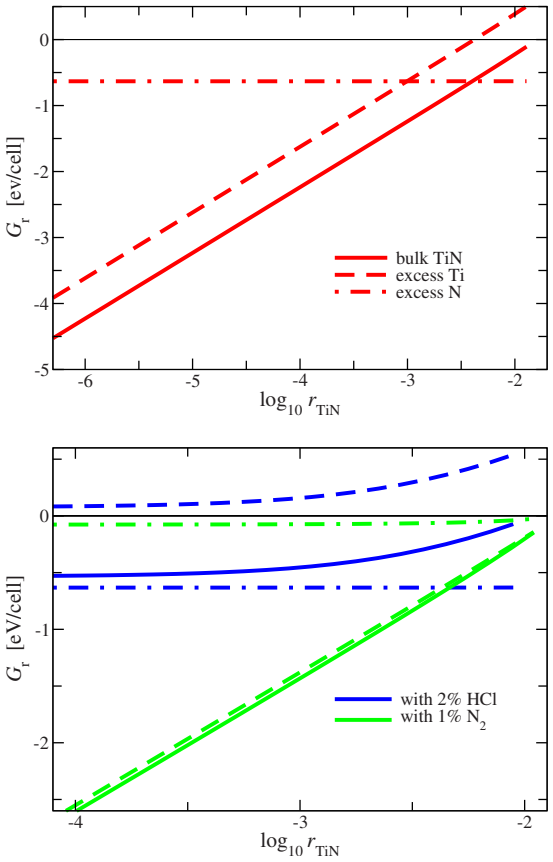

FIG. 6. (Color online) Free energies of reaction G_r of CVD bulk TiN, excess Ti and excess N layers at the TiX(111) surface as a function of the scaled reaction rate r_{TiN}. In the top panel, experimental values (Ref. 37) for the supply gas compositions from are used, see also main text. Temperature and pressure are chosen as in Fig. 5. The termination critically depends on the scaled deposition rate. The bottom panel illustrates the effect of varying deposition parameters. For bulk, excess Ti, and excess N, the same line style as in the upper panel applies. Blue (dark) lines correspond to an HCl concentration of 2% in the supply gas. Green (light) lines correspond to the case where the N_2 concentration is decreased to 1% and the temperature is raised to $T=1200$ °C. In both cases, the changes are assumed to be balanced by the H_2 concentration. An increased HCl concentration leads to a N-terminated surface, independently the value of r_{TiN}. A decreased N_2 concentration favors Ti termination.

dynamic equilibrium, that is, for $r_{TiN} \ll r_{TiN}^{crit}$, we have $G_r^{TiN/N} > G_r^{TiN/Ti}$. In this regime, a Ti-terminated surface is more favorable. Close to dynamic equilibrium, that is, for $r_{TiN} \sim r_{TiN}^{crit}$, we have $G_r^{TiN/N} < G_r^{TiN/Ti}$. Furthermore, $G_r^{TiN/Ti}$ is positive there. In this regime, a N-terminated surface is more favorable.

In the lower panel we illustrate the effects of varying the deposition parameters. Assuming an increased HCl content in the supply gas, balanced by the H_2 content, we find that $G_r^{TiN/Ti}$ turns positive over the whole range of the scaled reaction rate. Thus, we predict a N-terminated TiN(111) surface. Conversely, a decrease of the N_2 concentration in the supply gas (balanced by H_2) and a simultaneous increase of the deposition temperature, to $T=1200$ °C results into the favorization of a Ti-terminated surface.

In summary, we find that, under the conditions specified in Ref. 34, the as-deposited TiC(111) surface will be Ti terminated. Forcing a C-terminated surface by variation of process parameters within the specified supply gas cannot be achieved. Under the conditions specified in Ref. 37, the TiN(111) surface can, in principle, be either Ti- or N-terminated, depending on the ratio r_{TiN} between the deposition and supply rate. By introducing a slight amount of HCl into the supply gas, a N-terminated surface will be forced. With another choice of deposition parameters a Ti-terminated surface will evolve.

VI. DISCUSSION

The AIT-DG method that we have proposed in Sec. III and illustrated in Sec. V is designed to describe surface terminations as a function of the growth environment. Our predictions are based on calculations of the free energies of reaction G_{r}. We motivate this criterion by the physical principle that all systems strive for the states of low energy, given relevant boundary conditions. The method applies in dynamic equilibrium but also in scenarios where (dynamic) equilibrium is not maintained but the system still settles into a steady state. The method assumes that kinetic effects do not lock the system into thermodynamically unstable morphologies. It assumes in essence that a high deposition temperature causes a continuous annealing of the emerging structure.

A. Model limitations

Kinetic-barrier effects certainly exist and may prevent some systems from actually reaching the structure and morphology with the lowest thermodynamic energy.[19] Similar to the AIT-SE method, our method neglects these barrier effects. In principle, this approximation limits the applicability of our method to high-temperature growth where barriers become less important. Nevertheless, kinetic effects cannot be expected to alter the predictions in cases similar to TiC. This is because one of the free energies of reaction is negative (Ti excess) while the other is positive (C excess).

Another obvious limitation is that of the ideal-gas approximation from which we infer the temperature and pressure dependence of the molecular chemical potentials. Formally this approximation limits our description to low-pressure scenarios but the approach could easily be generalized by a more refined description of the gas thermodynamics.

B. Growth and rate equations

Our method is capable of describing surface terminations as they evolve during a growth process. This is fundamentally different from predicting the termination of a surface that is in equilibrium with the environment. As illustrated for TiN in the top panel of Fig. 6, the emerging surface termination depends on the scaled reaction rate, $r_{\mathrm{Ti}X}=R_{\mathrm{Ti}X}/R_{\mathrm{sup}}$. In such cases, our method should have clear advantages over the AIT-SE method. Use of our method requires only that measurements of the scaled reaction rate are made available.[53]

We are dealing with an open system that has both a gas flow and a consumption of gases during deposition. In a closed system, where the number of gas-phase species is fixed, the surface-gas system will approach equilibrium (unless there are important kinetic barriers).[28] Similarly, the growing surface and the gas environment could be in a state of dynamic equilibrium. In this case, the analysis in Sec. III F shows how the AIT-SE formalism could be extended to cover a description of the deposition. This can even work for materials that do not contain constituents A for which there exist molecular counterparts A_n.[47] Using the free surface energy as equilibrium predictor, the chemical potentials of atoms in the gas can be associated as an appropriate difference between molecular chemical potentials. An explicit example for TiC in an CH_4-$TiCl_4$-H_2 environment is given in Eq. (12). However, since the chemical potentials of atoms now depend on partial pressures of several gas-phase species, there is still a need to determine all relevant partial pressures. The rate-equation approach presented here supplies the information that is necessary for application of either the AIT-SE or the more general AIT-DG description of deposition growth.[54]

We emphasize that growing systems, in general, do not need to reach dynamic equilibrium but may be in any other steady state (if steady state is reached at all). If dynamic equilibrium was always maintained, the scaled reaction rate $r_{\mathrm{Ti}X}$ would always assume its critical value, that is, a maximum. The absolute deposition rate could then be increased to arbitrarily large values, simply by increasing the supply rate at a fixed total pressure. We believe that the assumption of dynamic equilibrium is too optimistic for CVD systems and we would not generally trust dynamic-equilibrium descriptions. The here-proposed theory of deposition growth (AIT-DG) applies also when the deposition and supply rates are independent variables.

C. Innovation potential

Using the free energy of reaction for the formation of excess layers on a specified surface we have shown for Ti*X*(111) how surface terminations can be understood from knowledge of the details of the CVD gas supply. For TiN, we have also illustrated that the method can be used to guide the growth toward a desired surface composition. That is, we have shown that we can modify the deposition environment (supply gas composition, deposition temperature, and deposition pressure) to allow either of the two surface terminations to emerge.

From this point of view our suggested method has a potential for accelerating innovation.[13] In the case of Ti*X*(111), the potential to design the surface termination may seem trivial. The change from a Ti- to a N-terminated TiN(111) surface that follows from raising the HCl concentration in the supply gas could likely also be obtained by, terminating the deposition process with an replacement of the $TiCl_4$-N_2-H_2 supply gas with a pure N_2 supply gas. We argue, however, that our method is valuable for characterizing more complex materials with a larger variety of possible surface terminations. This is particularly true when we extend the application to understand binding at interfaces that arise

in deposition growth,[55] for example, in the case of thin-film alumina on TiC.[56]

VII. SUMMARY AND CONCLUSIONS

We present a method based on *ab initio* calculations supported by thermochemical data to predict terminations of surfaces as they emerge during high-temperature deposition growth from a multicomponent gas, for example, chemical vapor deposition. The method describes scenarios that are located between a static equilibrium and the fully nonequilibrium regime that requires a complete kinetic description. It relies on the basic thermodynamical principle that all systems strive for low-energy states subject to statistics and other boundary conditions. Rate equations and associated steady-state solutions play a central role in the calculation of free energies of reaction. We use the latter to determine the chemical composition of the outermost surface layer of the growing surface.

We illustrate the approach for TiX(111) (X=C or N). For TiC, we predict a Ti-terminated surface when fabricated under the conditions stated in Ref. 34. For TiN, our predictions based on experimental conditions reported in Ref. 37 are not so clear. We find that the termination depends on the ratio between the reaction rate and the rate at which the gas is supplied to the reaction chamber.[57] In or close to dynamic equilibrium, we predict a N-terminated TiN surface. Departing from dynamic equilibrium will result in a Ti-terminated surface. We also suggest deposition parameters for which Ti- or N-terminated surfaces can be achieved independent of reaction and supply rates.

We also compare our method with the AIT-SE method.[15,16] We show that the predictions of our method agree with those of the AIT-SE method in the limit where (dynamic) equilibrium is maintained but also point out that this condition is not necessarily applicable to growth. In a closed system (absence a gas flow), there is an affinity to reach equilibrium. In an open system (with the gas flow turned on), one could expect a corresponding affinity to reach dynamic equilibrium. However, as discussed in Sec. VI, this expectation is likely too optimistic for general CVD growth conditions. In such cases, our method has clear advantages since it does not *a priori* implement equilibrium constraints.

The choice of materials, in particular TiC, also exemplifies the broader applicability of our method as compared to a strict implementation of the AIT-SE method.[47] Our method is not formally limited to predictions of oxide surface stability (or as in extensions of AIT-SE, to A_mB_n compound surfaces for which there is an A_k or B_k counterpart in the gas phase).

Finally the capability of predicting different surface terminations as a function of the deposition conditions illustrates the predictive power of our method. It motivates continued development of *ab initio* thermodynamics, also in a role to guide experimental optimization of surface and interfacial structures.

ACKNOWLEDGMENTS

We thank T. S. Rahman and Z. Konkoli for encouraging discussions during preparation of the manuscript. Support from the Swedish National Graduate School in Materials Science (NFSM), from the Swedish Foundation for Strategic Research (SSF) through ATOMICS, from the Swedish Research Council (VR) and from the Swedish National Infrastructure for Computing (SNIC) is gratefully acknowledged.

APPENDIX: GIBBS FREE ENERGY OF FORMATION AS PREDICTOR OF SURFACE TERMINATIONS

Chemical reaction theory provides the basis to relate the probabilities P_A and P_B for A and B surface termination to free energies of reaction G_r. The surface transformations described by Eq. (5) can be cast into the following rate equations for the probability of growing either an A- or B-terminated surface

$$\partial_t P_A = -(\Gamma_b^I + \Gamma_f^{II})P_A + (\Gamma_f^I + \Gamma_b^{II})P_B, \tag{A1a}$$

$$\partial_t P_B = (\Gamma_b^I + \Gamma_f^{II})P_A - (\Gamma_f^I + \Gamma_b^{II})P_B. \tag{A1b}$$

The steady-state solution is $P_A/P_B=(\Gamma_f^I+\Gamma_b^{II})/(\Gamma_b^I+\Gamma_f^{II})$ where $\Gamma_{\{f,b\}}^{\{I,II\}}$ are forward (f) and backward (b) reaction rates identified inreactions (5a) and (5b). These rates can be expressed as the products of the corresponding microscopic rate constants $k_{\{f,b\}}^{\{I,II\}}$, and of an environment-specific product $Q_{\{f,b\}}=\Pi_i[X_i]^{\nu_{\{f,b\},i}^{\{I,II\}}}$, Refs. 28 and 29. Here $[X_i]$ denotes the concentration of molecule X_i and $\nu_{\{f,b\},i}^{\{I,II\}}$ is the (positively counted) stoichiometric coefficient as reactant (f) and product (b) in reaction (5a) or (5b). We note that $Q_{\{f,b\}}$ is strictly speaking a product of activities from all parts in the reactions (5a) and (5b) but for surfaces (or solid) the activity can be approximated by unity.

The general relation $\beta G_r=-\ln K+\ln Q$ with β the inverse temperature, relates G_r to the equilibrium constant $K=k_f/k_b$ and $Q=Q_b/Q_f$. We have $Q_{\{f,b\}}^{\{I,II\}}=\Gamma_{\{f,b\}}^{\{I,II\}}/k_{\{f,b\}}$ and find $\exp(-\beta[G_r^A-G_r^B])=\Gamma_f^I\Gamma_b^{II}/(\Gamma_b^I\Gamma_f^{II})$.

Dynamic equilibrium is characterized by $G_r^A+G_r^B=0$ or equivalently $\Gamma_f^I\Gamma_f^{II}/(\Gamma_b^I\Gamma_b^{II})=1$, from which it follows that

$$P_A/P_B|_{\text{dyn.eq.}} = \exp(-\beta[G_r^A - G_r^B]/2). \tag{A2}$$

Away from dynamic equilibrium, this relation may not hold exactly. However, within a broad range of nonequilibrium conditions we may still approximate the arithmetric mean $[\langle x,y\rangle_{AM}=(x+y)/2]$ in $P_A/P_B=\langle\Gamma_f^I,\Gamma_b^{II}\rangle_{AM}/\langle\Gamma_b^I,\Gamma_f^{II}\rangle_{AM}$ by the geometric mean $[\langle x,y\rangle_{GM}=(xy)^{1/2}]$ expressing $\exp(-\beta[G_r^A-G_r^B]/2)=\langle\Gamma_f^I,\Gamma_b^{II}\rangle_{GM}/\langle\Gamma_b^I,\Gamma_f^{II}\rangle_{GM}$. This suggests that the evaluation in Eq. (6) remains a good approximate measure of relative surface termination also out of equilibrium.

*rohrer@chalmers.se

[1] I. Chorkendorff and J. W. Niemantsverdriet, *Concepts in Modern Catalysis and Kinetics*, 2nd ed. (WILEY-VCH, Weinheim, 2007).

[2] W. Weiss and W. Ranke, Prog. Surf. Sci. **70**, 1 (2002).

[3] N. Camillone III, K. Adib, J. P. Fitts, K. T. Rim, G. W. Flynn, S. A. Joyce, and R. M. Osgood, Surf. Sci. **511**, 267 (2002).

[4] J. Schoiswohl, G. Tzvetkov, F. Pfuner, M. G. Ramsey, S. Surnev, and F. P. Netzer, Phys. Chem. Chem. Phys. **8**, 1614 (2006).

[5] J. R. Kitchin, J. K. Nørskov, M. A. Barteau, and J. G. Chen, Catal. Today **105**, 66 (2005).

[6] Z. Łodziana and J. K. Nørskov, J. Chem. Phys. **115**, 11261 (2001).

[7] A. Vojvodic, Licentiate thesis, Chalmers University of Technology and University of Göteborg, 2006.

[8] T. L. Einstein and T. J. Stasevich, Science **327**, 423 (2010).

[9] C. Stampfl, M. V. Ganduglia-Pirovano, K. Reuter, and M. Scheffler, Surf. Sci. **500**, 368 (2002); *Handbook of Materials Modeling*, edited by Sidney Yip (Springer, Berlin, 2005), Vol. 1, pp. 149–194; P. Ruggerone, C. Ratsch, and M. Scheffler, *Growth and Properties of Ultrathin Epitaxial Layers*, The Chemical Physics of Solid Surfaces Vol. 8, edited by D. A. King and D. P. Woodruff (Elsevier, Amsterdam, 1997), pp. 490–544.

[10] J. K. Nørskov, T. Bligaard, J. Rossmeisl, and C. H. Christensen, Nat. Chem. **1**, 37 (2009); B. Hammer and J. K. Nørskov, Adv. Catal. **45**, 71 (2000).

[11] B. I. Lundqvist, A. Bogicevic, S. Dudiy, P. Hyldgaard, S. Ovesson, C. Ruberto, E. Schröder, and G. Wahnström, Comput. Mater. Sci. **24**, 1 (2002); B. I. Lundqvist, A. Bogicevic, K. Carling, S. V. Dudiy, S. Gao, J. Hartford, P. Hyldgaard, N. Jacobson, D. C. Langreth, N. Lorente, S. Ovesson, B. Razaznejad, C. Ruberto, H. Rydberg, E. Schröder, S. I. Simak, G. Wahnström, and Y. Yourdshahyan, Surf. Sci. **493**, 253 (2001).

[12] G. Makov, C. Gattioni, and A. DeVita, Model. Simul. Mater. Sci. Eng. **17**, 084008 (2009); R. M. Nieminen, J. Phys.: Condens. Matter **14**, 2859 (2002); M. W. Finnis, *ibid.* **8**, 5811 (1996); P. C. Weakliem and E. A. Carter, J. Chem. Phys. **98**, 737 (1993).

[13] For example, as discussed in T. S. Rahman, J. Phys.: Condens. Matter **21**, 080301 (2009); Ø. Borck, P. Hyldgaard, and E. Schröder, Phys. Rev. B **75**, 035403 (2007).

[14] E. Kaxiras, Y. Bar-Yam, J. D. Joannopoulos, and K. C. Pandey, Phys. Rev. B **35**, 9625 (1987).

[15] I. G. Batyrev, A. Alavi, and M. W. Finnis, Phys. Rev. B **62**, 4698 (2000).

[16] K. Reuter and M. Scheffler, Phys. Rev. B **65**, 035406 (2001).

[17] W. Zhang, J. R. Smith, and X. G. Wang, Phys. Rev. B **70**, 024103 (2004).

[18] K. E. Tan, M. W. Finnis, A. P. Horsfield, and A. P. Sutton, Surf. Sci. **348**, 49 (1996).

[19] S. Ovesson, A. Bogicevic, and B. I. Lundqvist, Phys. Rev. Lett. **83**, 2608 (1999).

[20] A. Bogicevic, S. Ovesson, B. I. Lundqvist, and D. R. Jennison, Phys. Rev. B **61**, R2456 (2000).

[21] P. Kratzer, E. Penev, and M. Scheffler, Appl. Phys. A: Mater. Sci. Process. **75**, 79 (2002).

[22] O. Trushin, A. Karim, A. Kara, and T. S. Rahman, Phys. Rev. B **72**, 115401 (2005).

[23] As exemplified by X. G. Wang, A. Chaka, and M. Scheffler, Phys. Rev. Lett. **84**, 3650 (2000); A. Marmier and S. C. Parker, Phys. Rev. B **69**, 115409 (2004); J. Ahn and J. W. Rabalais, Surf. Sci. **388**, 121 (1997).

[24] As exemplified by A. Stierle, F. Renner, R. Streitel, H. Dosch, W. Drube, and B. C. Cowie, Science **303**, 1652 (2004); G. Kresse, M. Schmid, E. Napetschnig, M. Shishkin, L. Kohler, and P. Varga, *ibid.* **308**, 1440 (2005).

[25] As exemplified by W. Zhang and J. R. Smith, Phys. Rev. B **61**, 16883 (2000); J. Mayer, C. P. Flynn, and M. Rühle, Ultramicroscopy **33**, 51 (1990).

[26] J. R. Arthur, Surf. Sci. **500**, 189 (2002).

[27] H. O. Pierson, *Handbook of Chemical Vapor Deposition* (Noyes, New York, 1992).

[28] Y. Demirel, *Nonequilibrium Thermodynamics: Transport and Rate Processes in Physical, Chemical and Biological Systems*, 2nd ed. (Elsevier, Amsterdam, 2007).

[29] N. Tschoegl, *Fundamentals of Equilibrium and Steady-State Thermodynamics*, 1st ed. (Elsevier, Amsterdam, 2000).

[30] T. Q. Li, S. Noda, Y. Tsuji, T. Ohsawa, and H. Komiyama, J. Vac. Sci. Technol. A **20**, 583 (2002).

[31] P. Komninou, G. P. Dimitrakopulos, G. Nouet, T. Kehagias, P. Ruterana, and Th. Karakostas, J. Phys.: Condens. Matter **12**, 10295 (2000).

[32] R. Hillel, M. Maline, F. Gourbilleau, G. Nouet, R. Carles, and A. Mlayah, Mater. Sci. Eng., A **168**, 183 (1993).

[33] A. Vojvodic, A. Hellman, C. Ruberto, and B. I. Lundqvist, Phys. Rev. Lett. **103**, 146103 (2009).

[34] M. Halvarsson, H. Norden, and S. Vuorinen, Surf. Coat. Technol. **61**, 177 (1993).

[35] We note, however, that both are stoichiometric films in the limit of a large thickness.

[36] S. Ruppi and A. Larsson, Thin Solid Films **388**, 50 (2001).

[37] A. Larsson and S. Ruppi, Thin Solid Films **402**, 203 (2002).

[38] C. Ruberto and B. I. Lundqvist, Phys. Rev. B **75**, 235438 (2007).

[39] A. Vojvodic, C. Ruberto, and B. I. Lundqvist, Surf. Sci. **600**, 3619 (2006).

[40] M. Aono, C. Oshima, S. Zaima, S. Otani, and Y. Ishizawa, Jpn. J. Appl. Phys., Part 2 **20**, L829 (1981).

[41] C. Oshima, M. Aono, S. Zaima, Y. Shibata, and S. Kawai, J. Less-Common Met. **82**, 69 (1981).

[42] S. Zaima, Y. Shibata, H. Adachi, C. Oshima, S. Otani, M. Aono, and Y. Ishizawa, Surf. Sci. **157**, 380 (1985).

[43] The (total) free energy per bulk unit is conveniently defined as $g_{TiX}=\lim_{n\to\infty} G_{TiX}(n+1)-G_{TiX}(n)$ where n is the number of bilayers in the TiX slab. Since the bulk energy does not depend on the actual surface termination, we could also replace $G_{TiX}(n+1)$ by $G_{TiX/Ti}(n+1)$ or $G_{TiX/X}(n+1)$ if we simultaneously replace $G_{TiX}(n)$ by $G_{TiX/Ti}(n)$ or $G_{TiX/X}(n)$, respectively.

[44] We note that we could have chosen nonstoichiometric slabs as initial configurations of the surface and adsorb additional layers on one of the two equivalent sides of this slab. In this case, we need to use a modified version of the definition of $G_r^{TiX/Ti}$. We emphasize, however, that the results presented here are independent of the choice of the definition of $G_r^{TiX/Ti}$, that is, both definitions are equivalent.

[45] *NIST-JANAF Thermochemical Tables*, M. W. Chase, Jr. (American Chemical Society/American Institute of Physics for the National Institute of Standards and Technology, Washington, D.C./New York, 1998).

[46] We are not aware of determinations of mean frequencies of Ti and X in TiX (X=C,N) which could directly enable an estimate

of the vibrational contributions similar to that given in Ref. 16. Because there is a large difference in masses between Ti and *X* one can expect a larger correction in the vibrational free energy for the lighter *X*. However, differences in such vibrational contributions will only shift the crossing points in the free energies of reaction and therefore not alter qualitative predictions or the value of the presented method.

[47] The AIT-SE formalism is essentially designed for oxides in equilibrium with an O_2-dominated environment. Here, we consider Ti*X* in a much more complicated environment. However, the above definitions, steps, and conclusions readily carry over to growth of an oxide in an environment that is more complex than a pure or O_2-dominated environment.

[48] B. Hammer, O. H. Nielsen, J. J. Mortensen, L. Bengtsson, L. B. Hansen, A. C. E. Madsen, Y. Morikawa, T. Bligaard, A. Christensen, and J. Rossmeisl, available from https://wiki.fysik.dtu.dk/dacapo

[49] D. Vanderbilt, Phys. Rev. B **41**, 7892 (1990).

[50] J. P. Perdew, J. A. Chevary, S. H. Vosko, K. A. Jackson, M. R. Pederson, D. J. Singh, and C. Fiolhais, Phys. Rev. B **46**, 6671 (1992).

[51] H. J. Monkhorst and J. D. Pack, Phys. Rev. B **13**, 5188 (1976).

[52] *NIST Computational Chemistry Comparison and Benchmark Database*, edited by R. D. Johnson (NIST Standard Reference Database, Gaithersburg, MD, 2006), Vol. 101, Release 14.

[53] In practice, measuring the exhaust rate R_{exh} (as a function of the supply rate R_{sup}) that is required to keep the total deposition pressure constant suffices to determine the scaled deposition rate.

[54] We note that rate equations may be required even in cases where the relevant atomic chemical potential can be determined from that of gases that are supplied and for which the concentrations in the supply gas is known. Equation (18) clearly shows that the steady-state concentrations will in general differ from the concentrations in the supply gas. Using experimental deposition parameters for TiN, we find that deviations in the steady-state pressure p_i from those that are expected from the concentration in the supply gas $p_i^0 = c_i \cdot p$ can become as large as 20%.

[55] J. Rohrer and P. Hyldgaard (unpublished).

[56] In a previous study, we have shown how direct application of AIT-SE yields a preference for formation of nonbinding TiC/alumina interfaces, in direct contradiction with the materials use as wear-resistant coatings, J. Rohrer, C. Ruberto, and P. Hyldgaard, J. Phys.: Condens. Matter **22**, 015004 (2010).

[57] This ratio is, in principle, accessible by monitoring the supply and exhaust rate at a fixed pressure.